Original Article

Pancreatic ductal adenocarcinoma with synchronous and metachronous hepatic metastasis predicted by contrast-enhanced ultrasound

Wan-Ying Jia[1], Yang Gui[1], Xue-Qi Chen[1], Li Tan[1], Jing Zhang[1], Meng-Su Xiao[1], Xiao-Yan Chang[4], Xin-Ting Sang[2], Meng-Hua Dai[3], Jun-Chao Guo[3], Chun-Mei Bai[5], Yue-Juan Cheng[5], Jing-Lin Li[1], Xin Yang[1], Jian-Chu Li[1], Yu-Xin Jiang[1], Ke Lv[1]

[1]Department of Ultrasound, Peking Union Medical College Hospital, Chinese Academy of Medical Sciences and Peking Union Medical College, Beijing, China; [2]Department of Liver Surgery, Peking Union Medical College Hospital, Chinese Academy of Medical Sciences and Peking Union Medical College, Beijing, China; [3]Department of General Surgery, Peking Union Medical College Hospital, Chinese Academy of Medical Sciences and Peking Union Medical College, Beijing, China; [4]Department of Pathology, Peking Union Medical College Hospital, Chinese Academy of Medical Sciences and Peking Union Medical College, Beijing, China; [5]Department of Medical Oncology, Peking Union Medical College Hospital, Chinese Academy of Medical Sciences and Peking Union Medical College, Beijing, China

Contributions: (I) Conception and design: WY Jia, K Lv; (II) Administrative support: XT Sang, MH Dai, JC Li, YX Jiang; (III) Provision of study materials or patients: L Tan, J Zhang, MS Xiao, XY Chang, YJ Cheng; (IV) Collection and assembly of data: Y Gui, XQ Chen, YJ Cheng, CM Bai; (V) Data analysis and interpretation: WY Jia, JL Li, X Yang, K Lv; (VI) Manuscript writing: All authors; (VII) Final approval of manuscript: All authors.

Correspondence to: Ke Lv. Department of Ultrasound, Peking Union Medical College Hospital, Chinese Academy of Medical Sciences and Peking Union Medical College, Beijing 100730, China. Email: lvke@163.com; Xin-Ting Sang. Department of Liver Surgery, Peking Union Medical College Hospital, Chinese Academy of Medical Sciences and Peking Union Medical College, Beijing 100730, China. Email: sangxt@pumch.cn; Meng-Hua Dai. Department of General Surgery, Peking Union Medical College Hospital, Chinese Academy of Medical Sciences and Peking Union Medical College, Beijing 100730, China. Email: daim66@126.com.

Background: Contrast-enhanced ultrasound (CEUS) has proven valuable in diagnosing benign and malignant pancreatic diseases, but its value in evaluating hepatic metastasis remains to be further explored. This study investigated the relationship between CEUS features of pancreatic ductal adenocarcinoma (PDAC) and concomitant or recurrent liver metastases after treatment.

Methods: This retrospective study included 133 participants with PDAC who were diagnosed with pancreatic lesions with CEUS at Peking Union Medical College Hospital from January 2017 to November 2020. According to the CEUS classification methods in our center, all the pancreatic lesions were classified as either with rich or poor blood supply. Additionally, quantitative ultrasonographic parameters were measured in the center and periphery of all pancreatic lesions. CEUS modes and parameters of the different hepatic metastasis groups were compared. The diagnostic performance of CEUS was calculated for diagnosing synchronous and metachronous hepatic metastasis.

Results: The proportions of rich blood supply and poor blood supply were 46% (32/69) and 54% (37/69), respectively, in the no hepatic metastasis group; 42% (14/33) and 58% (19/33), respectively, in the metachronous hepatic metastasis (MHM) group; and 19% (6/31) and 81% (25/31), respectively, in the synchronous hepatic metastasis (SHM) group. The wash-in slope ratio (WIS ratio) between the center of the lesion and around the lesion and peak intensity ratio (PI ratio) between the center of the lesion and around the lesion had higher values in the negative hepatic metastasis group ($P<0.05$). In predicting synchronous and metachronous hepatic metastasis, the WIS ratio had the best diagnostic performance. The sensitivity (SEN), specificity (SPE), accuracy (ACC), positive predictive value (PPV), and negative predictive value (NPV) were 81.8%, 95.7%, 91.2%, 90.0%, and 91.7%, respectively, for MHM; and 87.1%, 95.7%, 93.0%, 90.0%, and 94.3%, respectively, for SHM.

Conclusions: CEUS would be helpful in image surveillance for synchronous or metachronous hepatic metastasis of PDAC.

Keywords: Contrast-enhanced ultrasound (CEUS); pancreatic ductal adenocarcinoma (PDAC); synchronous hepatic metastasis (SHM); metachronous hepatic metastasis; fibrosis (MHM)

Submitted Oct 16, 2022. Accepted for publication Apr 06, 2023. Published online Apr 24, 2023.
doi: 10.21037/qims-22-1132
View this article at: https://dx.doi.org/10.21037/qims-22-1132

Introduction

Pancreatic ductal adenocarcinoma (PDAC) is currently the third leading cause of cancer mortality in both men and women and has the worst 5-year survival rate of any cancer (1). The prognosis of PDAC is dismal, and the 5-year survival rate is only 8% for all stages combined. Surgical resection seems to be the only potentially curative treatment for PDAC. However, approximately 50% of patients present with distant metastases at the time of diagnosis, with synchronous hepatic metastasis (SHM) being associated with a poorer prognosis and a contraindication to surgery (2).

The poor prognosis of patients with PDAC is also closely related to early metastasis (3), of which metachronous hepatic metastasis (MHM) accounts for 60–90% (3-5) and is an independent factor for prognosis (6). The mean survival time and 5-year disease-specific survival of patients with MHM are significantly lower than those of patients with other metastatic types (7), and these patients require different therapeutic approaches (8). As mentioned above, evaluating hepatic metastasis is critical to clinical decision-making in PDAC.

The main imaging examinations for pancreatic lesions include ultrasound (US), computed tomography (CT), and magnetic resonance imaging (MRI). The detection rate of hepatic metastases by these methods is 60–81% (3). Despite advances in diagnostic imaging modalities, PDAC remains lethal and incurable in most cases. Moreover, it is more difficult to obtain satisfactory accuracy for tiny lesions or microscopic metastases that emerge after surgery (9), and MHM cannot be predicted. Therefore, how to identify patients with PDAC at risk of hepatic metastasis is an area of active research in imaging.

Conventional US is the preferred screening method due to its noninvasiveness and simplicity. Contrast-enhanced ultrasound (CEUS) has become an area of intense research interest in the field of US in recent years and is widely used because of its ability to visualize the microcirculation within a lesion. However, its main application is in the determination of the nature of the lesion, and there have been relatively fewer studies on liver metastases (10). The US contrast agent has a diameter of <10 μm and can freely pass through capillaries, which can effectively mimic the hemodynamic characteristics of red blood cells and visualize the tumor microcirculation. PDAC shows 2 types of enhancement in CEUS, hypo-enhancement and iso-enhancement, with the former being the most common and the difference between them being mainly related to its microenvironmental composition (10-13). Hypo-enhancement PDAC has more fibrous stroma and fewer microvessels, resulting in fewer vessels involved in the microcirculation and lesions showing hypo-enhancement. In contrast, iso-enhancement PDAC contains more glandular vesicle cells and less fibrous matrix, resulting in a higher number of vessels involved in the microcirculation (11,14,15). We speculated upon whether it is possible to show the different areas of perfusion in the lesion using CEUS, thus providing more information for the assessment of hepatic metastases in PDAC. Therefore, we attempted to examine the relationship between the CEUS mode and parameters of PDAC and synchronous and metachronous hepatic metastases. We present the following article in accordance with the STARD reporting checklist (available at https://qims.amegroups.com/article/view/10.21037/qims-22-1132/rc).

Methods

This study was conducted in accordance with the Declaration of Helsinki (as revised in 2013). The institutional review board of Peking Union Medical College Hospital approved the study (No. SK1733), and the requirement for individual consent for this retrospective analysis was waived.

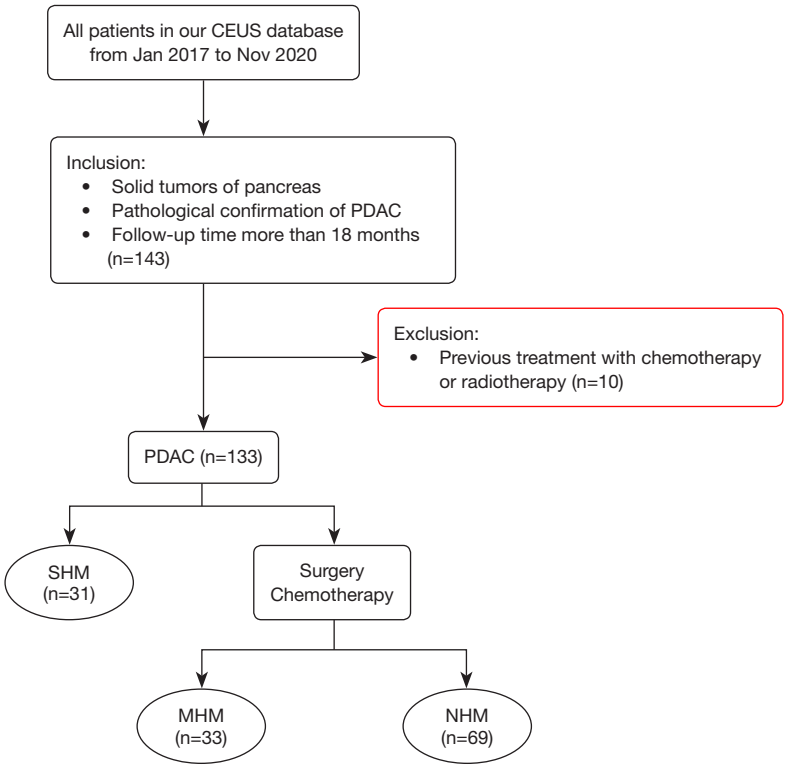

Figure 1 Flowchart of the study enrollment. CEUS, contrast-enhanced ultrasound; PDAC, pancreatic ductal adenocarcinoma; SHM, synchronous hepatic metastasis; MHM, metachronous hepatic metastasis; NHM, negative hepatic metastasis.

Patients

From January 2017 to December 2020, we retrospectively reviewed our study CEUS database (Peking Union Medical College Hospital, a single center) of patients. The inclusion criteria were as follows: (I) solid tumors of the pancreas; (II) PDAC pathologically confirmed by surgical resection, percutaneous biopsy, or endoscopic ultrasound biopsy; and (III) a follow-up duration of more than 18 months. The exclusion criterion was previous treatment with chemotherapy or radiotherapy (*Figure 1*).

Patients with PDAC were followed up every 3 months. Follow-up routines included liver function tests [alanine aminotransferase (ALT), aspartate aminotransferase (AST), etc.], serum tumor marker detection, US, and contrast-enhanced computed tomography (CECT). When CECT was still unable to determine the nature of the liver mass, dynamic MRI ^{18}F-fluorodeoxyglucose (^{18}F-FDG) positron emission tomography-computed tomography (PET-CT) imaging was chosen.

CEUS technique

All patients were asked to fast for at least 8 hours before CEUS. All US examinations were performed with a Philips iU22 unit (Philips Medical Systems, Bothell, WA, USA), using a 5 to 7-MHz linear transducer for the baseline examination and contrast study. For lesions in the tail of the pancreas that could not be easily displayed, the patient was asked to lie in the right decubitus position and undergo examination by oblique section scan under the right rib to achieve better examination results.

First, the pancreas was examined for the location of the suspicious lesion on the grayscale US. Color Doppler was performed to evaluate intralesional vascularity. The probe was fixed with a sectorial swing during the examination. The plane with the maximum suspicious lesion and normal pancreatic parenchyma was selected for the CEUS examination. Then, the mechanical index (MI) was set at 0.05–0.08 for the CEUS examination. The US contrast agent SonoVue (Bracco, Milan, Italy) was dissolved in 5 mL

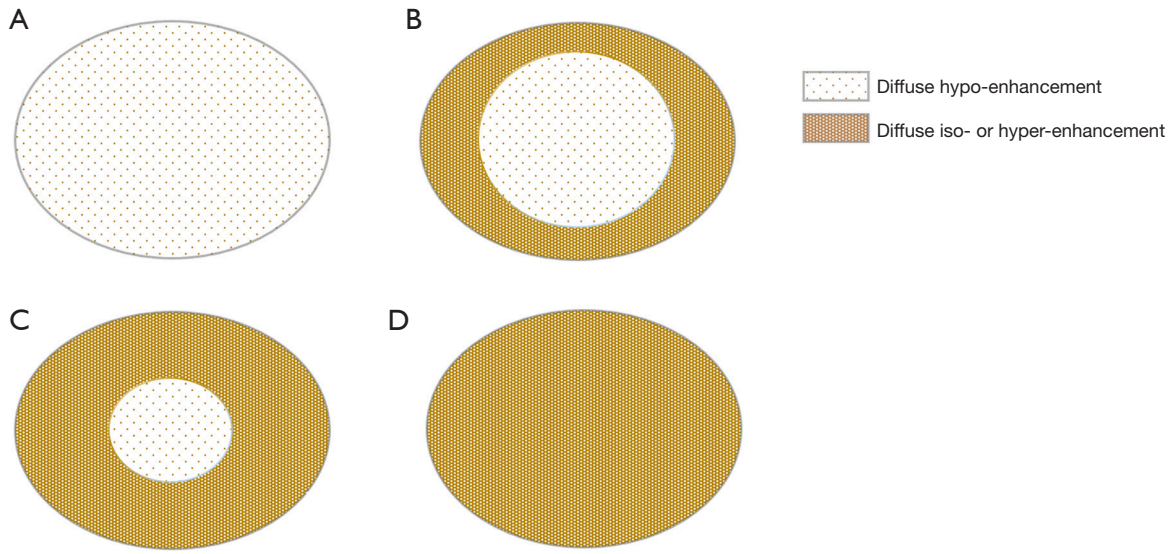

Figure 2 CEUS mode. (A) Poor blood supply: diffuse hypo-enhancement. (B) Poor blood supply: diffuse hypo-enhancement greater than 50%. (C) Rich blood supply: diffuse hypo-enhancement less than 50%. (D) Rich blood supply: diffuse iso-enhancement or hyperenhancement. CEUS, contrast-enhanced ultrasound.

of saline according to the manufacturer's instructions. The routine CEUS protocol for the pancreas at our institution includes grayscale US and CEUS. A fast bolus injection of 2.4 mL of contrast agent was administered intravenously and followed by 5 mL of saline. The patient was told to maintain a stationary posture continuously so that the dynamic perfusion process of the lesion could be observed in real time. The duration was 2 min and 30 s. All enhanced dynamic images were saved in AVI format.

Image interpretation: qualitative analysis

The enhancement mode of pancreatic lesions was analyzed by 2 radiologists with more than 5 years of experience in pancreatic imaging. According to the European Federation of Societies for Ultrasound in Medicine and Biology (EFSUMB) guidelines (10), the CEUS process was divided into the arterial and venous phases, defined as ≤30 and 31–120 s after injection of the contrast agent, respectively.

PDAC enhancement was classified as an iso-enhancement pattern (lesion enhancement equal to that of the surrounding pancreatic parenchyma), or hypo-enhancement pattern (lesion enhancement lower than that of the surrounding pancreatic parenchyma) in the arterial phase. Following this, all patients were divided, according to the naked eye, into 2 CEUS modes distinguished by the distribution of enhancement degree of pancreatic lesions: (I) poor blood supply mode (*Figure 2A*,*2B*)—the arterial phase shows a diffuse hypo-enhancement area in the center of the tumor with an area greater than 50%, or the entire tumor shows diffuse hypo-enhancement; and (II) rich blood supply mode (*Figure 2C*,*2D*)—the arterial phase shows a diffuse hypo-enhancement area in the center of the tumor with an area less than 50% or the entire tumor shows diffuse iso-enhancement. If there was a discrepancy between the 2 radiologists, agreement was reached by consensus.

Time-intensity curve analysis of CEUS images: quantitative analysis

CEUS images were imported into offline QLAB version 4.2 advanced software (Philips Medical Systems, Bothell, WA, USA). The first step was to delineate the actual size of the lesion, as the size of the lesion shown in the grayscale images may contain areas of necrosis, inflammation, and so on. We defined the area of fast wash-out in the venous phase of CEUS as the actual size of the pancreatic lesion. In the second step, regions of interest (ROIs) were placed in the center and around the lesion (*Figure 3*). The center and around ROIs were selected to the same depth as far as possible. The area immediately adjacent to the lesion, but still entirely within the lesion, was defined as the boundary (*Figure 3B*,*3G*,*3J*; the blue dashed box is the central ROI and the orange dashed box is the surrounding ROI). Finally,

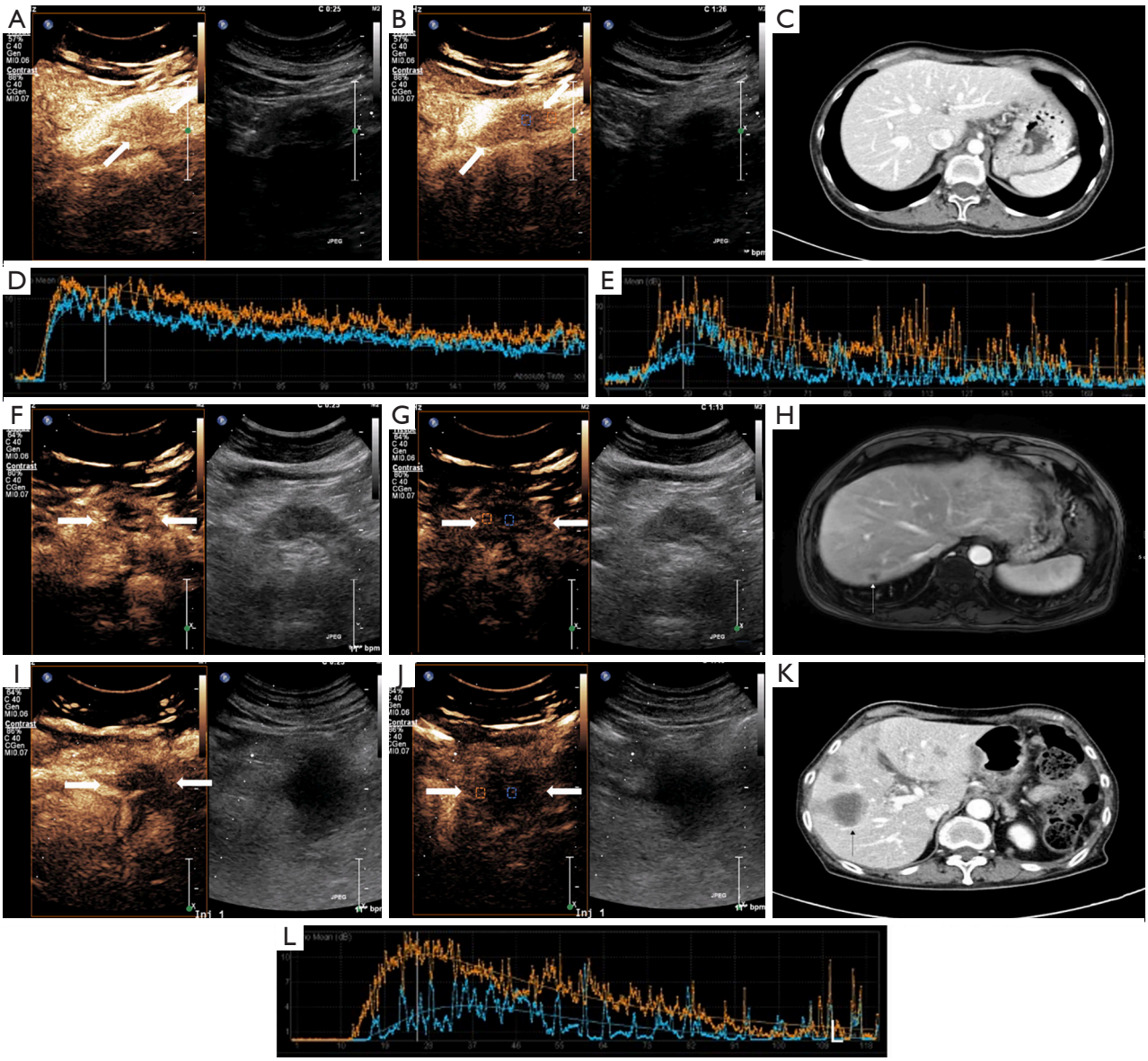

Figure 3 CEUS images of blood supply mode and parameters of PDAC in different hepatic metastasis groups. (A-D) A 56-year-old female with PDAC in the NHM group. Arterial phase (A) and late phase (B) of rich blood supply mode CEUS images. (C) CECT image showing no metastases in the liver. (D) TIC image with a WIS ratio of 0.88 and a PI ratio of 0.72. (E-H) A 70-year-old female with PDAC in the MHM group. Arterial phase (F) and late phase (G) of rich blood supply mode CEUS images. (H) CE-MRI image showing metachronous metastases in the liver (thin white arrow). (E) TIC image with a WIS ratio of 0.60 and a PI ratio of 0.62. (I-L) A 54-year-old male with PDAC in the SHM group. Arterial phase (I) and late phase (J) of rich blood supply mode CEUS images. (K) CECT image showing synchronous metastases in the liver (thin black arrow). (L) TIC image showing a WIS ratio of 0.42 and a PI ratio of 0.41. (A,B,F,G,I,J) The lesion is marked by a white arrow. (B,G,J) The blue dashed box shows the placement of the ROI in the center of the lesion, and the orange dashed box shows the placement of the ROI around the lesion. CEUS, contrast-enhanced ultrasound; PDAC, pancreatic ductal adenocarcinoma; NHM, negative hepatic metastasis; CECT, contrast-enhanced computed tomography; TIC, time-intensity curve; WIS, wash-in slope; PI, peak intensity; MHM, metachronous hepatic metastasis; CE-MRI, contrast-enhanced magnetic resonance imaging; SHM, synchronous hepatic metastasis; ROI, region of interest.

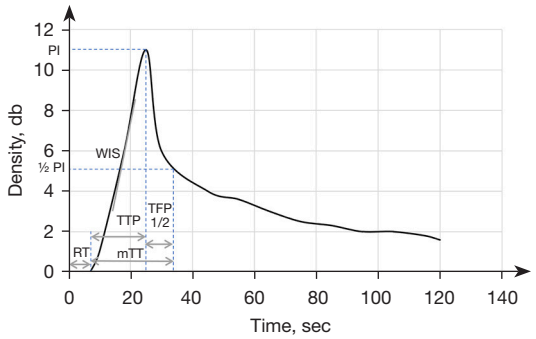

Figure 4 CEUS TIC parameter diagram. WIS: wash-in slope, base to peak ascending slope. TTP: time to peak from the beginning of enhancement to maximum intensity. PI: peak intensity, maximum intensity. MTT: mean transit time from the beginning of enhancement to the decrease to half of the maximum intensity. TFP1/2, time from peak to 1/2 from maximum power to half of the maximum intensity; RT, rise time from the injection of contrast agent to the beginning of enhancement; CEUS, contrast-enhanced ultrasound; TIC, time-intensity curve.

each frame was examined using the QLAB software; frames where the lesion was out of the ROI due to the patient's respiratory movements were removed, and time-intensity curves (TICs; the specific definitions of curve parameters are given in the *Figure 4* footnote) and quantitative parameters of the tumor tissue were obtained.

After obtaining the values of all quantitative parameters, we divided the values between the center and the surrounds of the lesion to obtain the ratio of each parameter: wash-in slope (WIS) ratio = $WIS_{center}/WIS_{surrounds}$, peak intensity (PI) ratio = $PI_{center}/PI_{surrounds}$, time to peak (TTP) ratio = $TTP_{center}/TTP_{surrounds}$, mean transit time (mTT) ratio = $mTT_{center}/mTT_{surrounds}$, time from peak to 1/2 (TFP1/2) ratio = $TFP1/2_{center}/TFP1/2_{surrounds}$, and rise time (RT) ratio = $RT_{center}/RT_{surrounds}$. The TIC parameters were independently measured by the 2 abovementioned radiologists and averaged after consistency was evaluated by intraclass correlation coefficient (ICC). Radiologists were blinded to the final results.

Statistical analysis

The chi-squared analysis of variance (ANOVA) and z test were performed to analyze group differences. Interobserver variability for the TIC parameters measurements of the 2 readers was analyzed by calculating the ICC (0.00–0.20 poor, 0.21–0.40 fair, 0.41–0.60 moderate, 0.61–0.80 good, and 0.81–1.00 excellent correlation). To predict synchronous and metachronous hepatic metastasis, the sensitivity (SEN), specificity (SPE), positive predictive value (PPV), negative predictive value (NPV), accuracy (ACC), and receiver operating characteristic (ROC) were calculated. A P value of less than 0.05 was considered significant for all tests. The statistical analysis was performed using SPSS version 22.0 (IBM Corp., Armonk, NY, USA).

Results

Clinical characteristics

A total of 133 patients were enrolled in this study and divided into 3 groups: (I) 69 in the no hepatic metastasis group (NHM; median follow-up period of 19 months), (II) 33 in the MHM group (median follow-up period of 10 months: 3 diagnosed with dynamic MRI and 30 diagnosed with CECT), and (III) 31 in the SHM group (1 diagnosed by pathology and 30 diagnosed with CECT). The detailed demographics and clinical characteristics are described in *Table 1*. Tumor-node-metastasis (TNM) stage (16) showed statistically significant differences among the 3 groups ($P<0.05$). For the TNM stage, there were substantial differences between the SHM group and the NHM group but not in the MHM group. Patients in the NHM and MHM groups were mainly in stages II and III. As for the therapy, there was no statistical difference between the NHM group and MHM groups, and both involved surgical treatment and chemotherapy. The SHM group was statistically different from the other 2 groups in terms hepatic metastases, which could only be treated with chemotherapy. There were no statistically significant differences in sex, age, location, pancreatic duct width, or carbohydrate antigen 19-9 (CA19-9) level.

CEUS mode and TIC parameter analyses

The CEUS mode and TIC parameters in different hepatic metastasis groups are described in *Table 2* and *Figure 3*. The CEUS mode differed significantly among the 3 groups ($P<0.05$). Intragroup comparisons only showed significant differences between the NHM and SHM groups. In the NHM group, the proportion of patients with rich blood supply was 46% (32/69), and that of those with poor blood supply was 54% (37/69). In the SHM group, the proportion of patients with rich and poor blood supply was 19% (6/31) and 81% (25/31), respectively (*Figure 5A*). In

Table 1 Tumor presenting features and patient characteristics of the 3 groups

Characteristic	No hepatic metastasis (n=69)	Metachronous hepatic metastasis (n=33)	Synchronous hepatic metastasis (n=31)	P value
Sex				0.77
Male	41 (59.4)	21 (63.6)	17 (54.8)	
Female	28 (40.6)	12 (36.4)	14 (45.2)	
Age, years	59.91±8.97	59.91±8.54	59.03±9.72	0.89
TNM (initial)				<0.05
I	5 (7.3)	4 (12.2)	0 (0)	
II	33[a] (47.8)	18[a] (54.5)	0 (0)	
III	31[a] (44.9)	11[a] (33.3)	0 (0)	
IV	0[a] (0)	0[a] (0)	31 (100.0)	
Size (cm)	4.09±0.14	4.30±0.21	4.54±0.23	0.23
Location				0.85
Head	30 (43.5)	16 (48.5)	13 (41.9)	
Body/tail	39 (56.5)	17 (51.5)	18 (58.1)	
Pancreatic duct width (cm)	0.22±0.03	0.28±0.05	0.25±0.04	0.53
CA19-9				0.16
Negative	15 (21.7)	7 (21.2)	2 (6.5)	
Positive	54 (78.3)	26 (78.8)	29 (93.5)	
Therapy (initial)				<0.05
Surgery	18[a] (26.1)	11[a] (33.3)	0 (0)	
Chemo	51[a] (73.9)	22[a] (66.7)	31 (100.0)	

[a], the same letters indicate that the z test shows no statistical difference between the 2 groups. Values are presented as the mean ± standard deviation (SD) or number (%). TNM, tumor-node-metastasis stage; CA19-9, carbohydrate antigen 19–9.

Table 2 CEUS mode and parameters distinguishing different groups of hepatic metastases

CEUS index	No hepatic metastasis (n=69)	Metachronous hepatic metastasis (n=33)	Synchronous hepatic metastasis (n=31)	ICC	P value
CEUS					<0.05
Rich blood supply	32 (46.4)[a]	14 (42.4)[ab]	6 (19.0)[b]		
Poor blood supply	37 (53.6)[a]	19 (57.6)[ab]	25 (81.0)[b]		
WIS ratio (dB/sec)	0.81±0.01	0.43±0.04[a]	0.36±0.04[a]	0.91	<0.05
TTP ratio (sec)	0.99±0.01	1.02±0.02	1.03±0.03	0.93	0.19
PI ratio (dB)	0.79±0.02	0.64±0.04[a]	0.55±0.05[a]	0.94	<0.05
MTT ratio (sec)	0.94±0.03	0.98±0.08	0.95±0.06	0.92	0.89
TTP1/2 ratio (sec)	0.93±0.04	1.05±0.08	0.95±0.04	0.91	0.24
RT ratio (sec)	0.98±0.04	1.01±0.04	1.04±0.03	0.90	0.32

[a,b], consistent labeling of letters indicates the z test showed no statistical difference between the 2 groups. Values are presented as the mean ± standard deviation (SD) or number (%). CEUS, contrast-enhanced ultrasound; ICC, intraclass correlation coefficient; WIS, wash-in slope; TTP, time to peak; PI, peak intensity; mTT, mean transit time; RT, rise time.

Table 3 Prediction of hepatic metastases

Characteristic	AUC	SEN (%)	SPE (%)	ACC (%)	PPV (%)	NPV (%)
Metachronous						
WIS ratio	0.90	81.8	95.7	91.2	90.0	91.7
PI ratio	0.74	66.7	95.7	86.3	88.0	85.7
Synchronous						
WIS ratio	0.92	87.1	95.7	93.0	90.0	94.3
PI ratio	0.72	74.2	81.2	79.0	63.9	87.5
CEUS mode	0.68	80.6	55.1	66.6	44.6	86.4

AUC, area under the curve; SEN, sensitivity; SPE, specificity; ACC, accuracy; PPV, positive predictive value; NPV, negative predictive value; WIS, wash-in slope; PI, peak intensity; CEUS, contrast-enhanced ultrasound.

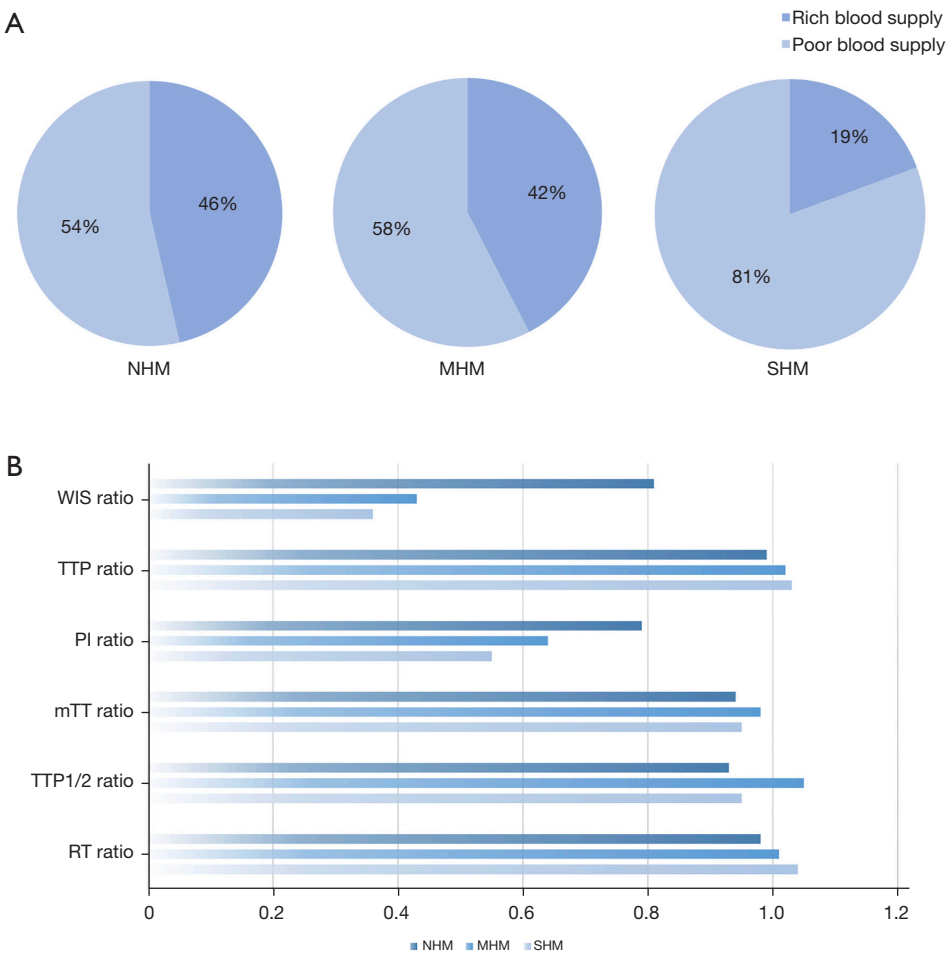

Figure 5 CEUS mode and parameters in different groups of hepatic metastases. (A) Distribution of CEUS mode in the different groups of hepatic metastases. (B) CEUS parameters in the different groups of hepatic metastases. WIS, wash-in slope; TTP, time to peak; PI, peak intensity; mTT, mean transit time; RT, rise time; CEUS, contrast-enhanced ultrasound; NHM, no hepatic metastasis; MHM, metachronous hepatic metastasis; SHM, synchronous hepatic metastasis.

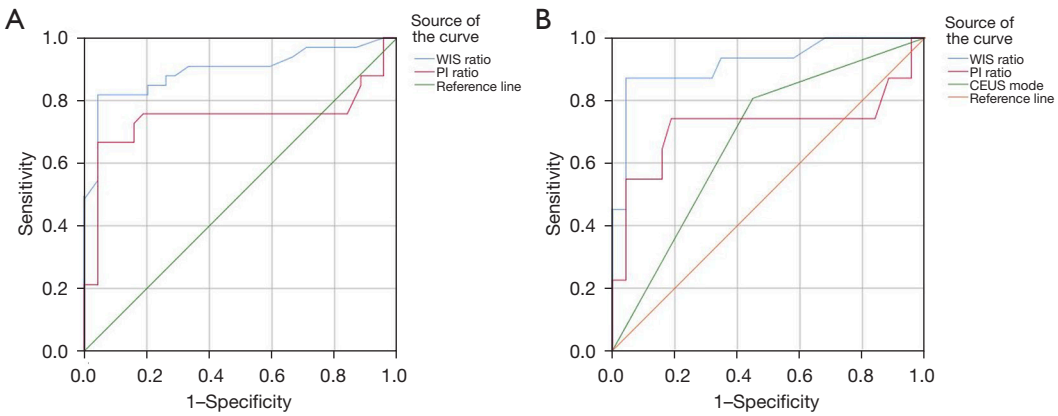

Figure 6 ROC curve for the presence of hepatic metastasis. (A) The ROC curve in diagnosing metachronous hepatic metastasis (WIS ratio: AUC =0.90; PI ratio: AUC =0.74). (B) The ROC curve in diagnosing synchronous hepatic metastasis (WIS ratio: AUC =0.92; PI ratio: AUC =0.72; CEUS mode: AUC =0.68). ROC, receiver operating characteristic; WIS, wash-in slope; AUC, area under the curve; PI, peak intensity; CEUS, contrast-enhanced ultrasound.

the CEUS parameter analyses, only the differences in WIS and PI ratios were statistically significant (P<0.05). Further intragroup comparisons showed that the differences in WIS and PI ratios were not statistically significant in the MHM and SHM groups. All of these parameters had higher values in the NHM group (*Figure 5B*). There were no significant differences in the TTP ratio, RT ratio, mTT ratio, or TFP1/2 ratio.

Prediction of hepatic metastasis

In predicting MHM using WIS ratio and PI ratio, WIS ratio had the best diagnostic performance. The area under curve (AUC), SEN, SPE, ACC, PPV, and NPV were 0.90, 81.8%, 95.7%, 91.2%, 90.0%, and 91.7%, respectively. In predicting SHM, WIS ratio still had the best diagnostic performance. The AUC, SE, SP, ACC, PPV, and NPV were 0.92, 87.1%, 95.7%, 93.0%, 90.0%, and 94.3%, respectively (*Table 3*, *Figure 6*).

Discussion

With the development of US technology, CEUS has played an essential role in diagnosing PDAC (10,11,17). Compared to CECT, which uses iodine or gadolinium technology for contrast imaging (11), CEUS uses microbubbles in pure blood pool imaging, which, with a diameter of less than 10 μm, can freely pass through capillaries, effectively simulating the hemodynamic properties of red blood cells. This technique has the advantage of real-time observation and realistic response to microvascular changes and is more conducive to the presentation of the microcirculation of the lesion. Moreover, this *in vivo* blood flow information is difficult to provide through pathological sections, so a greater number of studies can be conducted with the help of CEUS.

Our results showed that the CEUS mode and quantitative parameters differed among the different hepatic metastasis groups in PDAC (*Figure 5*), where the WIS ratio may be an important factor in assessing the risk of hepatic metastasis. The presence of hepatic metastases is an important independent prognostic factor for PDAC (18). Unfortunately, in current medical developments, it can only be accurately assessed at the time of surgery. Yokoyama *et al.* found that some patients with PDAC developed hepatic micrometastases during surgery, and the rate of hepatic metastases within 6 months after surgery in these patients was as high as 88% (19). This finding suggests that patients with hepatic metastases undergo microscopic changes that are not visible to the naked eye early in the course of the disease and incidentally confirms the reliability of the present study for predicting hepatic metastases in patients with PDAC from the perspective of microcirculation. According to previous studies (20-22), PDAC, as a tumor with a lack of blood supply, consists of more fibrous stroma and fewer microvessels. We hypothesized that PDAC in the group without hepatic metastasis had more acinar cells and loose fibrous stroma. In contrast, in the hepatic metastasis group, the closer the lesion was to the center, the more extracellular matrix was secreted. The microvessels were compressed, making it difficult for the contrast agent

to enter, leading to a difference in the WIS ratio. As for the physical barrier, a large amount of fibrous matrix can prevent the chemotherapeutic drugs from functioning, which is another important factor for the occurrence of hepatic metastasis in such patients at a later stage (15,23-25). The CEUS model can precisely reflect the characteristics of the microenvironment of PDAC from a macroscopic perspective, and its parameters can, to a certain extent, be used as quantitative indicators to capture the changes in the microenvironment more sensitively. We believe this is why the WIS ratio is better at predicting hepatic metastasis. Related *in vitro* studies demonstrated that the degree of fibrous stroma in the primary foci of pancreatic cancer was significantly higher in mice with a higher proportion of hepatic metastases than in mice without hepatic metastases (23), providing a pathological explanation for the results of this study. However, whether the WIS ratio can be used as an evaluation indicator for monitoring neoadjuvant treatment of PDAC remains to be further investigated.

Currently, research on risk assessment protocols for hepatic metastases from PDAC is still in progress. CA19-9 is the only peripheral blood-based biomarker used to diagnose PDAC, but some studies (26,27) have concluded that this marker is not tumor-specific and is not suitable as a diagnostic biomarker for early metastases. However, some studies (28-30) have shown a possible correlation between CA19-9 ≥400 U/mL and hepatic metastasis. Meanwhile, other studies (27,31,32) have shown that the presence of circulating tumor cells (CTCs) in portal blood is associated with a higher rate of liver metastasis after resection of the primary tumor. Mehdorn *et al.* found significant differences in proteins involved in immune cell chemotaxis and migration and cell growth in the serum of patients with early- and late-stage hepatic metastases (27). Li *et al.* used the clinicopathological characteristics of patients with PDAC to build artificial intelligence-based predictive models for the risk of hepatic metastasis (33). As for imaging, Zambirinis *et al.* performed preoperative CT-enhanced scans in patients with PDAC and found that radiomics could predict early hepatic metastasis in PDAC (34). Compared to previous studies (27,33,34), our study used a more convenient and radiation-free CEUS, which increases the use of available ultrasonographic information without adding additional burden to the patient. It thus provides a new way to assess the risk of hepatic metastasis from PDAC.

This study's findings indicated there to be no correlation between the occurrence of hepatic metastasis and the location of the primary pancreatic tumor. The prevalence of hepatic metastasis of PDAC is still in the research stage and currently remains controversial. Some scholars believe that liver metastasis of PDAC is not related to the location of the primary lesion (19), which is consistent with the results of our study. However, Kovač *et al.* asserted that the incidence of metastatic disease in patients with primary tumors located in the tail of the pancreas is significantly higher, and the bottom of the pancreas is denser, making metastasis easier (35). Therefore, this view needs to be further explored by analyzing a large amount of data.

Hepatic metastasis affects the therapeutic measures and prognosis of patients with PDAC. Identifying imaging factors that influence hepatic metastasis in PDAC is essential for better risk classification of patients and the development of treatment strategies. Our study showed that the quantitative parameter WIS ratio in CEUS is important in assessing the risk of hepatic metastasis. Therefore, neoadjuvant chemotherapy can be promoted for patients with PDAC at high risk of hepatic metastasis, when clinically assessed as necessary, to improve patient survival. Moreover, the frequency of follow-up for these patients can be increased to achieve early detection and early intervention to prolong the survival cycle. Our study not only expands the research horizons of pancreatic CEUS but also provides more useful information concerning the clinical follow-up treatment of patients with PDAC.

Nevertheless, our study had several limitations. First, we used a retrospective study design and conducted the study in a single center with a relatively small sample size. Second, not all patients with hepatic metastases had pathologic evidence. However, all patients had radiographic and clinically validated hepatic metastases. Third, further prospective clinical studies are needed to validate our results.

Conclusions

In the pretreatment US evaluation of PDAC, the mode and parameters of pancreatic CEUS may provide more helpful information concerning the hepatic metastasis of PDAC. A rich blood supply is more likely to occur in patients without hepatic metastasis. The WIS ratio is a key predictor of hepatic metastasis in PDAC. These features would be helpful in image surveillance for synchronous or metachronous hepatic metastasis of PDAC.

Acknowledgments

Funding: This work was funded by the National High-

Level Hospital Clinical Research Funding (No. 2022-PUMCH-B-065), the National Natural Science Foundation of China (Nos. 81873902 and 82171968), and the Peking Union Medical College Hospital Precipitation Fund (No. ZC201903600).

Footnote

Reporting Checklist: The authors have completed the STARD reporting checklist. Available at https://qims.amegroups.com/article/view/10.21037/qims-22-1132/rc

Conflicts of Interest: All authors have completed the ICMJE uniform disclosure form (available at https://qims.amegroups.com/article/view/10.21037/qims-22-1132/coif). The authors have no conflicts of interest to declare.

Ethical Statement: The authors are accountable for all aspects of the work in ensuring that questions related to the accuracy or integrity of any part of the work are appropriately investigated and resolved. This study was conducted in accordance with the Declaration of Helsinki (as revised in 2013). The institutional review board of Peking Union Medical College Hospital approved the study (No. SK1733), and individual consent for this retrospective analysis was waived.

References

1. Siegel RL, Miller KD, Fuchs HE, Jemal A. Cancer statistics, 2022. CA Cancer J Clin 2022;72:7-33.
2. De Dosso S, Siebenhüner AR, Winder T, Meisel A, Fritsch R, Astaras C, Szturz P, Borner M. Treatment landscape of metastatic pancreatic cancer. Cancer Treat Rev 2021;96:102180.
3. Tsilimigras DI, Brodt P, Clavien PA, Muschel RJ, D'Angelica MI, Endo I, Parks RW, Doyle M, de Santibañes E, Pawlik TM. Liver metastases. Nat Rev Dis Primers 2021;7:27.
4. Nielsen SR, Quaranta V, Linford A, Emeagi P, Rainer C, Santos A, Ireland L, Sakai T, Sakai K, Kim YS, Engle D, Campbell F, Palmer D, Ko JH, Tuveson DA, Hirsch E, Mielgo A, Schmid MC. Macrophage-secreted granulin supports pancreatic cancer metastasis by inducing liver fibrosis. Nat Cell Biol 2016;18:549-60.
5. Mou Y, Song Y, Liu J, Song H, Liu X, Li J, Ke N. Long Term Outcomes of No-Touch Isolation Principles Applied in Pancreaticoduodenectomy for Treatment of Pancreatic Adenocarcinoma: A Multicenter Retrospective Study with Propensity Score Matching. J Clin Med 2023;12:632.
6. Groot VP, Rezaee N, Wu W, Cameron JL, Fishman EK, Hruban RH, Weiss MJ, Zheng L, Wolfgang CL, He J. Patterns, Timing, and Predictors of Recurrence Following Pancreatectomy for Pancreatic Ductal Adenocarcinoma. Ann Surg 2018;267:936-45.
7. Zaborienė I, Strakšytė V, Ignatavičius P, Barauskas G, Dambrauskienė R, Žvinienė K. Dynamic Contrast-Enhanced Magnetic Resonance Imaging for Measuring Perfusion in Pancreatic Ductal Adenocarcinoma and Different Tumor Grade: A Preliminary Single Center Study. Diagnostics (Basel) 2023;13:521.
8. Jin T, Dai C, Xu F. Surgical and local treatment of hepatic metastasis in pancreatic ductal adenocarcinoma: recent advances and future prospects. Ther Adv Med Oncol 2020;12:1758835920933034.
9. Zeeshan MS, Ramzan Z. Current controversies and advances in the management of pancreatic adenocarcinoma. World J Gastrointest Oncol 2021;13:472-94.
10. Sidhu PS, Cantisani V, Dietrich CF, Gilja OH, Saftoiu A, Bartels E, et al. The EFSUMB Guidelines and Recommendations for the Clinical Practice of Contrast-Enhanced Ultrasound (CEUS) in Non-Hepatic Applications: Update 2017 (Short Version). Ultraschall Med 2018;39:154-80.
11. Jia WY, Gui Y, Chen XQ, Zhang XQ, Zhang JH, Dai MH, Guo JC, Chang XY, Tan L, Bai CM, Cheng YJ, Li JC, Lv K, Jiang YX. Evaluation of the diagnostic performance of the EFSUMB CEUS Pancreatic Applications guidelines (2017 version): a retrospective single-center analysis of 455 solid pancreatic masses. Eur Radiol 2022;32:8485-96.
12. Yan X, Lv K, Xiao M, Tan L, Gui Y, Zhang J, Chen X, Jia W, Li J. The diagnostic performance of contrast-enhanced ultrasound versus contrast-enhanced computed tomography for pancreatic carcinoma: a systematic review and meta-analysis. Transl Cancer Res 2022;11:3645-56.
13. Wang Y, Li G, Yan K, Fan Z, Long R, Shan J, Dai Y,

Wu W. Clinical value of contrast-enhanced ultrasound enhancement patterns for differentiating solid pancreatic lesions. Eur Radiol 2022;32:2060-9.
14. Aslan S, Nural MS, Camlidag I, Danaci M. Efficacy of perfusion CT in differentiating of pancreatic ductal adenocarcinoma from mass-forming chronic pancreatitis and characterization of isoattenuating pancreatic lesions. Abdom Radiol (NY) 2019;44:593-603.
15. Kim SI, Shin JY, Park JS, Jeong S, Jeon YS, Choi MH, Choi HJ, Moon JH, Hwang JC, Yang MJ, Yoo BM, Kim JH, Lee HW, Kwon CI, Lee DH. Vascular enhancement pattern of mass in computed tomography may predict chemo-responsiveness in advanced pancreatic cancer. Pancreatology 2017;17:103-8.
16. Chun YS, Pawlik TM, Vauthey JN. 8th Edition of the AJCC Cancer Staging Manual: Pancreas and Hepatobiliary Cancers. Ann Surg Oncol 2018;25:845-7.
17. Chen X, Hao F, Gui Y, Zhang J, Tan L, Xiao M, Zhang Q, Meng H, Li J, Jiang Y, Lv K. Enhancement patterns in the venous phase of contrast-enhanced ultrasounds: diagnostic value for patients with solid pancreatic lesions. Quant Imaging Med Surg 2021;11:4321-33.
18. Fanotto V, Salani F, Vivaldi C, Scartozzi M, Ribero D, Puzzoni M, Montagnani F, Leone F, Vasile E, Bencivenga M, De Manzoni G, Basile D, Fornaro L, Masi G, Aprile G. Primary Tumor Resection for Metastatic Colorectal, Gastric and Pancreatic Cancer Patients: In Search of Scientific Evidence to Inform Clinical Practice. Cancers (Basel) 2023;15:900.
19. Takesue S, Ohuchida K, Shinkawa T, Otsubo Y, Matsumoto S, Sagara A, et al. Neutrophil extracellular traps promote liver micrometastasis in pancreatic ductal adenocarcinoma via the activation of cancer associated fibroblasts. Int J Oncol 2020;56:596-605.
20. Gong XH, Xu JR, Qian LJ. Atypical and uncommon CT and MR imaging presentations of pancreatic ductal adenocarcinoma. Abdom Radiol (NY) 2021;46:4226-37.
21. Nakaoka K, Ohno E, Kawabe N, Kuzuya T, Funasaka K, Nakagawa Y, Nagasaka M, Ishikawa T, Watanabe A, Tochio T, Miyahara R, Shibata T, Kawashima H, Hashimoto S, Hirooka Y. Current Status of the Diagnosis of Early-Stage Pancreatic Ductal Adenocarcinoma. Diagnostics (Basel) 2023;13:215.
22. Kim H, Kim DH, Song IH, Kim B, Oh SN, Choi JI, Rha SE. Survival Prediction after Curative Resection of Pancreatic Ductal Adenocarcinoma by Imaging-Based Intratumoral Necrosis. Cancers (Basel) 2022;14:5671.
23. Endo S, Nakata K, Ohuchida K, Takesue S, Nakayama H, Abe T, et al. Autophagy Is Required for Activation of Pancreatic Stellate Cells, Associated With Pancreatic Cancer Progression and Promotes Growth of Pancreatic Tumors in Mice. Gastroenterology 2017;152:1492-1506.e24.
24. Roife D, Sarcar B, Fleming JB. Stellate Cells in the Tumor Microenvironment. Adv Exp Med Biol 2020;1263:67-84.
25. Zhou T, Tan L, Gui Y, Zhang J, Chen X, Dai M, Xiao M, Zhang Q, Chang X, Xu Q, Bai C, Cheng Y, Xu Q, Wang X, Meng H, Jia W, Lv K, Jiang Y. Correlation Between Enhancement Patterns on Transabdominal Ultrasound and Survival for Pancreatic Ductal Adenocarcinoma. Cancer Manag Res 2021;13:6823-32.
26. Hou J, Li X, Xie KP. Coupled liquid biopsy and bioinformatics for pancreatic cancer early detection and precision prognostication. Mol Cancer 2021;20:34.
27. Mehdorn AS, Gemoll T, Busch H, Kern K, Beckinger S, Daunke T, Kahlert C, Uzunoglu FG, Hendricks A, Buertin F, Wittel UA, Sunami Y, Röcken C, Becker T, Sebens S. Biomarkers in Liquid Biopsies for Prediction of Early Liver Metastases in Pancreatic Cancer. Cancers (Basel) 2022;14:4605.
28. Takagi C, Kikuchi Y, Shirakawa H, Hoshimoto S, Tomikawa M, Ozawa I, Hishinuma S, Ogata Y. Predictive Factors for Elevated Postoperative Carbohydrate Antigen 19-9 Levels in Patients With Resected Pancreatic Cancer. Anticancer Res 2019;39:3177-83.
29. Ren H, Wu CR, Aimaiti S, Wang CF. Development and validation of a novel nomogram for predicting the prognosis of patients with resected pancreatic adenocarcinoma. Oncol Lett 2020;19:4093-105.
30. Kondo N, Murakami Y, Uemura K, Nakagawa N, Takahashi S, Ohge H, Sueda T. Comparison of the prognostic impact of pre- and post-operative CA19-9, SPan-1, and DUPAN-II levels in patients with pancreatic carcinoma. Pancreatology 2017;17:95-102.
31. Tao L, Su L, Yuan C, Ma Z, Zhang L, Bo S, Niu Y, Lu S, Xiu D. Postoperative metastasis prediction based on portal vein circulating tumor cells detected by flow cytometry in periampullary or pancreatic cancer. Cancer Manag Res 2019;11:7405-25.
32. Hugenschmidt H, Labori KJ, Borgen E, Brunborg C, Schirmer CB, Seeberg LT, Naume B, Wiedswang G. Preoperative CTC-Detection by CellSearch® Is Associated with Early Distant Metastasis and Impaired Survival in Resected Pancreatic Cancer. Cancers (Basel) 2021;13:485.
33. Li Q, Bai L, Xing J, Liu X, Liu D, Hu X. Risk Assessment of Liver Metastasis in Pancreatic Cancer Patients Using

Multiple Models Based on Machine Learning: A Large Population-Based Study. Dis Markers 2022;2022:1586074.
34. Zambirinis CP, Midya A, Chakraborty J, Chou JF, Zheng J, McIntyre CA, Koszalka MA, Wang T, Do RK, Balachandran VP, Drebin JA, Kingham TP, D'Angelica MI, Allen PJ, Gönen M, Simpson AL, Jarnagin WR. Recurrence After Resection of Pancreatic Cancer: Can Radiomics Predict Patients at Greatest Risk of Liver Metastasis? Ann Surg Oncol 2022;29:4962-74.
35. Kovač JD, Mayer P, Hackert T, Klauss M. The Time to and Type of Pancreatic Cancer Recurrence after Surgical Resection: Is Prediction Possible? Acad Radiol 2019;26:775-81.

Cite this article as: Jia WY, Gui Y, Chen XQ, Tan L, Zhang J, Xiao MS, Chang XY, Sang XT, Dai MH, Guo JC, Bai CM, Cheng YJ, Li JL, Yang X, Li JC, Jiang YX, Lv K. Pancreatic ductal adenocarcinoma with synchronous and metachronous hepatic metastasis predicted by contrast-enhanced ultrasound. Quant Imaging Med Surg 2023;13(6):3902-3914. doi: 10.21037/qims-22-1132

